

Open camera or QR reader and  
scan code to access this article  
and other resources online.



# Basolateral Sorting of the Sodium/Iodide Symporter Is Mediated by Adaptor Protein 1 Clathrin Adaptor Complexes

Petrina Koumarianou,<sup>1,\*</sup> Celia Fernández-Méndez,<sup>1,\*</sup> Dánae Fajardo-Delgado,<sup>2</sup> Lidia Mirella Mielu,<sup>2,3</sup> Pilar Santisteban,<sup>1,3</sup> and Antonio De la Vieja<sup>2,3</sup>

**Background:** The sodium/iodide symporter (NIS) is a transmembrane protein located on the basolateral membrane of thyrocytes. Despite its physiological and clinical relevance, little is known about the mechanisms that mediate NIS subcellular sorting. In the present study, we examined NIS basolateral trafficking *in vitro* using non-thyroid and thyroid epithelial cells.

**Methods:** Immunofluorescence and Western blotting were performed to analyze NIS subcellular location and function in cells grown in monolayers under unpolarized and/or polarized conditions. Strategic NIS residues were mutated, and binding of NIS to clathrin adaptor complexes was determined by immunoprecipitation.

**Results:** We show that NIS reaches the plasma membrane (PM) through a thyrotropin-dependent mechanism 24 hours after treatment with the hormone. We demonstrate that NIS basolateral trafficking is a clathrin-mediated mechanism, in which the clathrin adaptor complexes AP-1 (A and B) sort NIS from the *trans*-Golgi network (TGN) and recycling endosomes (REs). Specifically, we show that the AP-1B  $\mu$ 1 subunit controls NIS basolateral sorting through common REs. In its absence, NIS is apically missorted but remains functional. Additionally, direct NIS basolateral transport from the TGN to the basolateral membrane is mediated by AP-1A through clathrin-coated vesicles that also carry the transferrin receptor. Loss of the  $\mu$ 1 subunit of AP-1A is functionally compensated by AP-1B. Furthermore, loss of both subunits diminishes NIS trafficking to the PM. Finally, we demonstrate that AP-1A binds to the L121 and LL562/563 residues on NIS, whereas AP-1B binds to L583.

**Conclusions:** Our findings highlight the novel involvement of the clathrin-coated machinery in basolateral NIS trafficking. Given that AP-1A expression is reduced in tumors, and its expression correlates with that of NIS, these findings will help uncover new targets in thyroid cancer treatment.

**Keywords:** AP-1A, AP-1B, clathrin, NIS trafficking, protein sorting, sodium iodide symporter

## Introduction

THE SODIUM/IODIDE SYMPORTER (NIS), encoded by the *SLC5A5* gene, mediates iodide uptake for the synthesis of thyroid hormones.<sup>1–4</sup> NIS is typically localized to the basolateral membrane of polarized thyroid follicular cells; however, it can be

expressed both at the basolateral membrane and at the apical membrane depending on its function in uptake or reabsorption, which are tissue-specific features.<sup>4–9</sup> NIS is mostly localized intracellularly in thyroid tumors, preventing successful radioiodide (RAI) therapy.<sup>7,9,10</sup> *SLC5A5* gene expression and NIS location in the membrane of thyroid follicular cells are positively regulated

<sup>1</sup>Instituto de Investigaciones Biomédicas “Alberto Sols”, Consejo Superior de Investigaciones Científicas (CSIC), Universidad Autónoma de Madrid, Madrid (UAM), Spain.

<sup>2</sup>Unidad de Tumores Endocrinos (UFIEC), Instituto de Salud Carlos III (ISCIII), Madrid, Spain.

<sup>3</sup>Ciber de Cáncer (CIBERONC), Instituto de Salud Carlos III (ISCIII), Madrid, Spain.

\*Both are co-first authors.

by thyrotropin (TSH) and other factors,<sup>9,11–15</sup> whereas activation of the RET-RAS-BRAF pathway suppresses NIS expression and membrane localization by different signaling cascades.<sup>16–18</sup>

While the crucial role of NIS location for its activity is well demonstrated,<sup>4</sup> the mechanism(s) underlying NIS trafficking to the basolateral and apical membrane remains enigmatic. A better understanding of the control of NIS expression and trafficking is important not only for thyroid gland physiology but also for recovering NIS function in cancer, which is critical for the success of ablative RAI. In this line, several proteins have been identified to interact with NIS and participate in thyroid cancer, including leukemia-associated RhoGEF (LARG),<sup>19</sup> pituitary tumor transforming gene binding factor,<sup>20,21</sup> ADP ribosylation factor 4 (ARF4),<sup>22</sup> and valosin-containing protein.<sup>22</sup>

Basolateral sorting signals are simple peptide motifs in the cytoplasmic domain of proteins that are recognized by adaptor proteins. This includes tyrosine, monoleucine, dileucine residues, and PDZ-binding motifs.<sup>23</sup> NIS is reported to have a PDZ target motif and three acidic dipeptide motifs in its C-terminus.<sup>24</sup> Intriguingly, the cytoplasmic C-terminus of NIS contains a dileucine motif that can be recognized by clathrin adaptors,<sup>24,25</sup> which might be involved in NIS trafficking.

Cytosolic adaptor proteins are components of protein coats associated with the *trans*-Golgi network (TGN) and/or recycling endosomes (REs), which may link cargo binding to clathrin.<sup>26</sup> The clathrin-associated adaptor protein 1 (AP-1) complex has a major role in clathrin-mediated basolateral sorting. AP-1 is a heterotetrameric complex that is present in two homologous isoforms, AP-1A and AP-1B, which share three of four subunits ( $\beta$ 1,  $\gamma$ , and  $\sigma$ ) and differ only in the subunits  $\mu$ 1A and  $\mu$ 1B, respectively.<sup>27</sup> Whereas AP-1A preferentially functions in biosynthetic routes, AP-1B sorts basolateral plasma membrane (PM) proteins in both biosynthetic and recycling routes.<sup>28–31</sup> In this regard, a recent study reported that AP-1B recognizes the NIS C-terminus.<sup>32</sup>

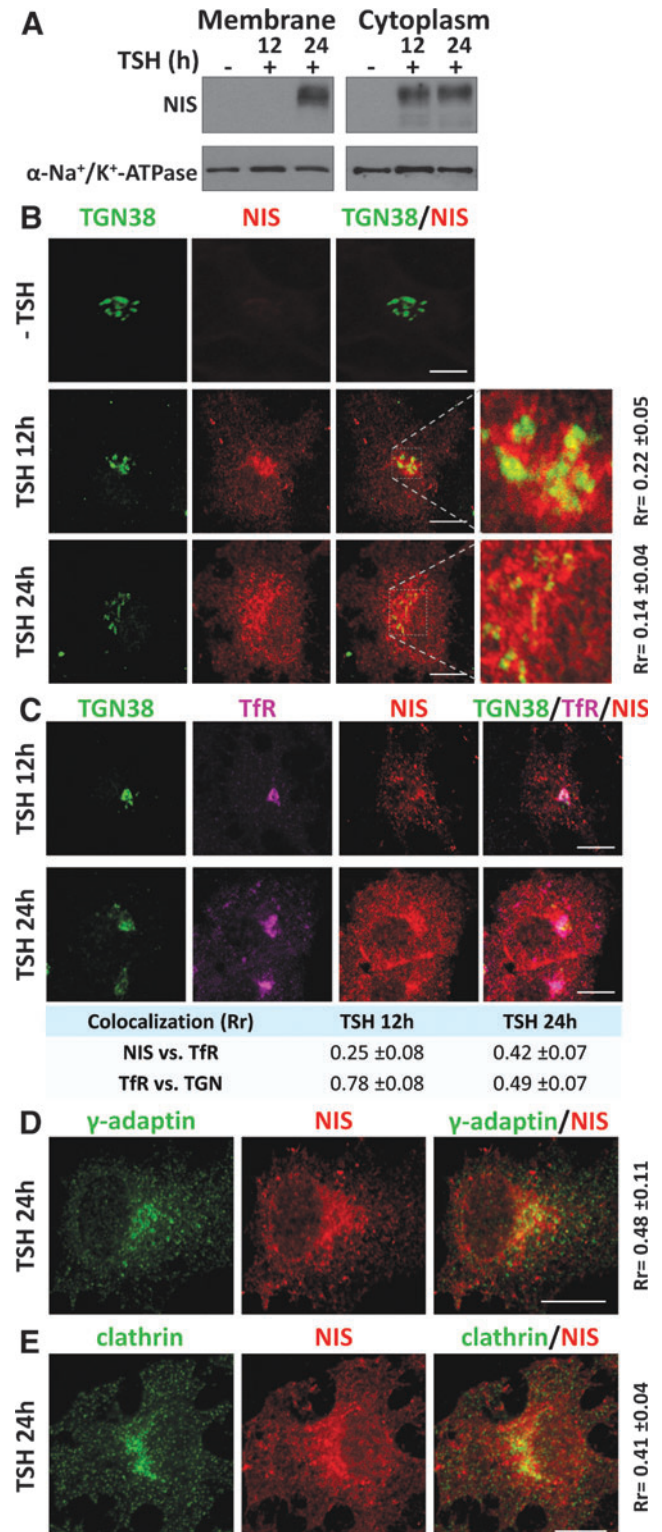
In this study, we sought to investigate the potential NIS-trafficking role of the adaptor protein complex AP-1 and to evaluate whether a clathrin-mediated pathway is responsible for NIS basolateral trafficking.

**FIG. 1.** Cellular localization of newly synthesized NIS in PCC13 cells after TSH induction and its localization within the TGN and recycling endosomes. (A) NIS protein expression by Western blotting of cytoplasmic and membrane-biotinylated extracts of PCC13 cells grown in medium without TSH during 5 days (–) and then stimulated with TSH for 12 and 24 hours.  $\alpha$ -Na<sup>+</sup>/K<sup>+</sup>-ATPase was used as a loading control. (B) Colocalization of NIS (red) with TGN38 (green) at the TGN in 5-day TSH-depleted PCC13 cells (–TSH) and after replenition with TSH for 12 and 24 hours. White squares mark an expanded area shown in the inset (right panels). (C) Triple colocalization confocal microscopy of NIS (red), TGN38 (green), and recycling endosome TfR (magenta) markers in PCC13 cells after 12 and 24 hours of TSH treatment. (D, E) Confocal immunofluorescence images of NIS colocalization with  $\gamma$ -adapting (D) and clathrin (E) after 24 hours of TSH treatment. Scale bars, 10  $\mu$ m. Quantitative colocalization analysis is indicated by Pearson's correlation coefficient ( $R_r$ ) and appears either in a blue table or in the lateral side of the colocalization images. More than 10 cells were analyzed in each case, and values are expressed in mean  $\pm$  SD. NIS, sodium/iodide symporter; TfR, transferrin receptor; TGN, *trans*-Golgi network; TSH, thyrotropin.

## Materials and Methods

### Cell culture, transfection, and immunofluorescence

Non-polarized rat PCC13 thyroid differentiated follicular cells and polarized Madin-Darby canine kidney (MDCK) cells were maintained as described.<sup>14,33</sup> Gene silencing, transfection, and immunofluorescence protocols are described in the Supplementary Data.



*Plasmids and site-directed mutagenesis*

Plasmids and primers used for site-directed mutagenesis are detailed in the Supplementary Data.

*Protein extraction and detection*

All experimental techniques for protein extraction and detection are described in the Supplementary Data.

*RAI transport assay and co-immunoprecipitation*

Polarized MDCK-hNIS and  $\mu$ 1AB-KD-hNIS cells were assayed for iodide transport as described,<sup>34</sup> with modifications detailed in the Supplementary Data.

**Results***NIS is trafficked from the TGN to the PM in clathrin-associated AP-1 vesicles and transferrin receptor-positive endosomes*

To characterize the basolateral sorting routes for NIS, we first assessed the subcellular location of newly synthesized NIS in cultured PCC13 cells upon TSH treatment. The absence of TSH led to the complete loss of NIS at the PM and cytoplasm (Fig. 1A), whereas its addition to the culture medium induced cytoplasmic NIS expression after 12 hours, which was detectable in the PM after 24 hours (Fig. 1A). Microscopy analysis revealed the presence of NIS in the TGN after 12 hours of TSH stimulation, as evidenced by its colocalization with the *trans*-Golgi protein TGN38 (Fig. 1B). NIS expression was also evident in the perinuclear region and cytoplasm, but not at the PM. NIS was confirmed at the PM after 24 hours of treatment, accompanied by a strong perinuclear and cytoplasmic distribution, and with little overlap with TGN38 (Fig. 1B). NIS labeling at a region close to the TGN suggested its association with REs, which transport cargo from the Golgi to the PM dependent on the clathrin-associated adaptor complex AP-1.<sup>28,35</sup>

NIS localization at REs was confirmed by analyzing the RE marker transferrin receptor (TfR), which is classically sorted by a clathrin-dependent mechanism. We observed an increase in NIS colocalization with TfR after 24 hours of TSH treatment, concomitant with a decline in colocalization between TfR and TGN38 (Fig. 1C).

Immunofluorescence analysis of NIS and the gamma subunit of AP-1 ( $\gamma$ -adapting) (Fig. 1D), as well as with clathrin (Fig. 1E), revealed colocalization at TGN/RE regions 24 hours after TSH supplementation, and a few areas of colocalization were also observed in the cytoplasm.

Overall, these results suggest that NIS exits the TGN and follows a clathrin-dependent biosynthetic pathway to the PM in thyroid follicular cells mediated by AP-1-coated vesicles and TfR-rich REs. Because  $\gamma$ -adapting is a common subunit of

AP-1A and 1B complexes, and TfR interacts with both at the TGN and at REs,<sup>31</sup> we explored the role of each clathrin adaptor variant in this process.

*NIS colocalizes with the  $\gamma$ ,  $\mu$ 1A, and  $\mu$ 1B subunits of AP-1 at the TGN and the perinuclear region*

To investigate where NIS basolateral sorting occurs, we performed immunofluorescence analysis for NIS and the TGN marker TGN46 in non-polarized MDCK cells overexpressing human NIS (MDCK-hNIS) (Fig. 2A). Quantitative colocalization analysis revealed a small overlap between NIS and TGN46, and NIS was also present at the perinuclear region and the PM. The intense NIS labeling at the perinuclear region, close to the TGN, again suggested its association with the REs that transport cargo from the Golgi to the PM dependent on AP-1 adaptors.<sup>28,35</sup>

We thus examined colocalization between NIS and the endogenous  $\gamma$ -adapting (Fig. 2B) in MDCK-hNIS cells also overexpressing  $\mu$ 1A (Fig. 2C) or  $\mu$ 1B (Fig. 2D) proteins. Confocal microscopy results showed a weak colocalization between  $\mu$ 1A and NIS at the TGN (white dots in the inset in Fig. 2C). Qualitative and quantitative analysis revealed small differences in colocalization between NIS and TGN46 (Fig. 2A) and overexpressed  $\mu$ 1B (Fig. 2D). Partial colocalization was also observed between the  $\mu$ 1B-positive compartment and the TGN (Fig. 2E).

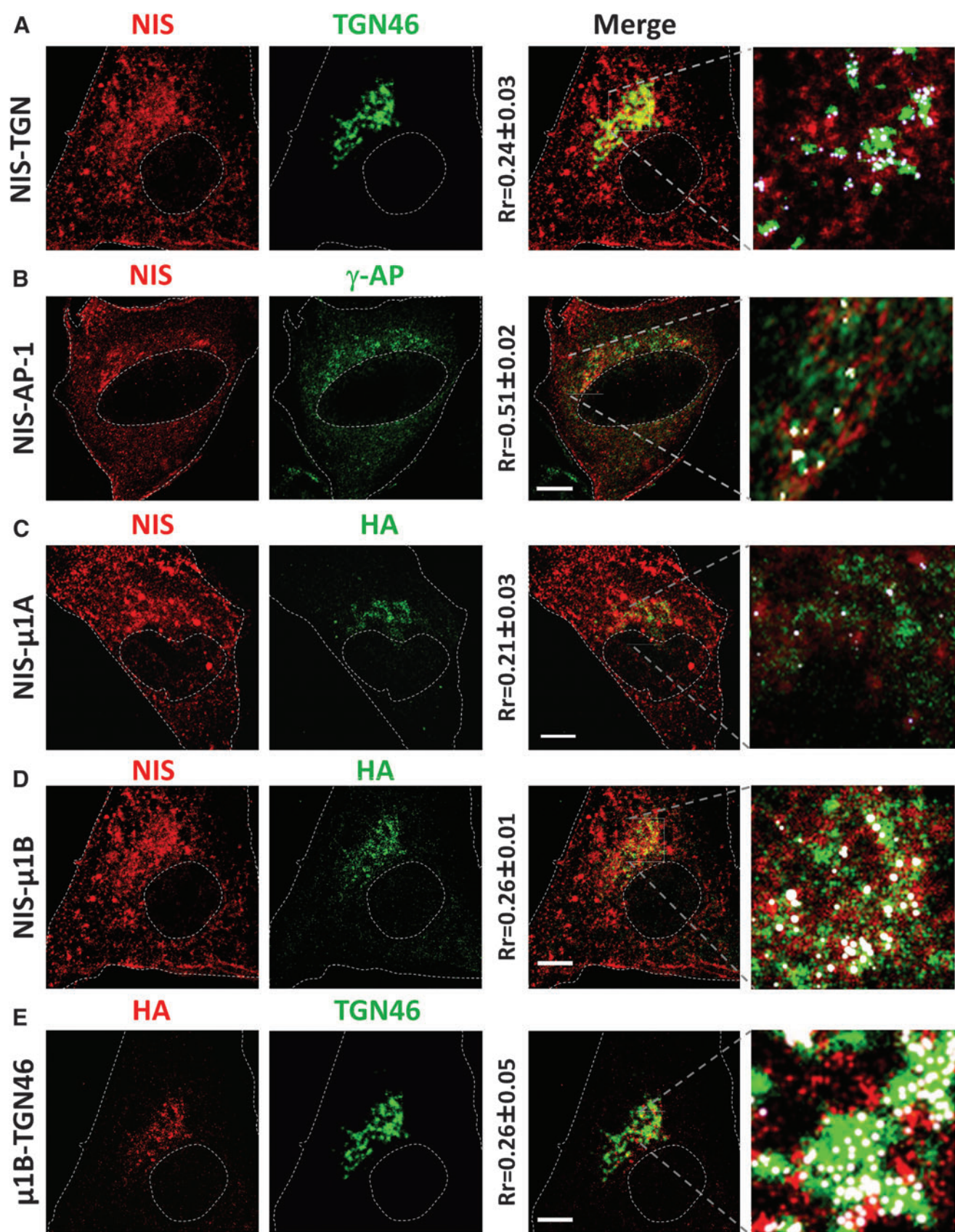
These data show that NIS colocalizes with AP-1A and AP-1B clathrin adaptor carriers at the TGN and RE, pointing to their involvement in NIS sorting.

*Knockdown of the AP-1A  $\mu$ 1A subunit has no effect on NIS basolateral membrane localization in polarized MDCK cells*

AP-1A controls trafficking from the TGN to the basolateral membrane by interactions between the subunit  $\mu$ 1A and cargo proteins through canonical and noncanonical motifs.<sup>30,31</sup> We assessed the role of AP-1A in NIS sorting by silencing the expression of  $\mu$ 1A in polarized MDCK-hNIS cells (grown on filters) (Fig. 3A). No changes were observed for basolateral NIS localization in polarized  $\mu$ 1A-KD-hNIS (50% silenced) cells compared with the steady-state basolateral NIS localization in control MDCK-hNIS cells (Fig. 3B). These findings were confirmed by biotinylation and Western blotting (Fig. 3C), which revealed a similar amount of NIS in the basolateral domain of both control (95%  $\pm$  3%) and  $\mu$ 1A-KD-hNIS (89%  $\pm$  7%) polarized cells and practically no apical NIS distribution. Basolateral membrane  $\alpha$ -Na<sup>+</sup>/K<sup>+</sup>-ATPase and apical membrane gp135 were analyzed to confirm polarization in  $\mu$ 1A-silenced cells (Fig. 3C).

**FIG. 2.** NIS colocalization with clathrin adaptors in MDCK cells. MDCK-hNIS cells were transfected with  $\mu$ 1A-HA or  $\mu$ 1B-HA vectors, and protein colocalization was analyzed by immunofluorescence after 48 hours. Shown are single representative confocal sections labeled with NIS (red), TGN46 (green), and HA (green/red). NIS colocalization with (A) TGN46, (B)  $\gamma$ -adapting ( $\gamma$ -AP), (C) clathrin adaptor subunits  $\mu$ 1A (HA), and (D)  $\mu$ 1B (HA). (E) TGN46 colocalization with  $\mu$ 1B (HA). Scale bars, 10  $\mu$ m. Regions of interest in white box are amplified, and colocalization points are shown as white dots in the inset (right panels). Quantitative colocalization analysis is indicated by Pearson's correlation coefficient ( $R_p$ ). More than 10 cells were analyzed in each case, and values are expressed in mean  $\pm$  SD. Dashed lines have been added to indicate the location of the edges of the nucleus and the PM. HA, human influenza hemagglutinin tag; MDCK, Madin-Darby canine kidney; PM, plasma membrane.





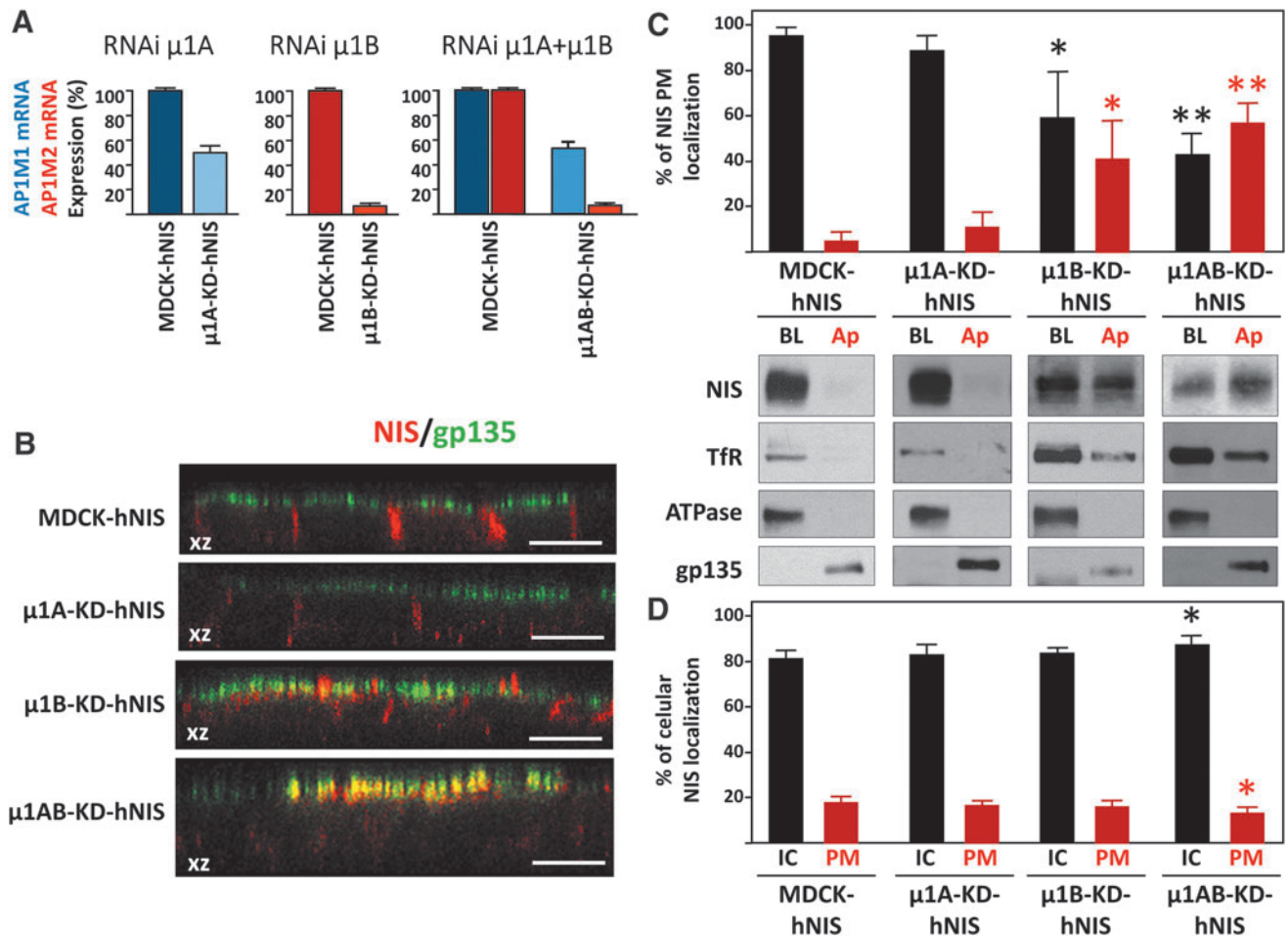


**FIG. 3.** NIS localization in the absence of  $\mu$ 1A,  $\mu$ 1B, or both. (A) *AP1M1* and/or *AP1M2* mRNA levels were determined by RT-qPCR in control MDCK-hNIS cells and in  $\mu$ 1A RNAi knockdown ( $\mu$ 1A-KD-hNIS),  $\mu$ 1B knockdown ( $\mu$ 1B-KD-hNIS), and  $\mu$ 1A+B knockdown ( $\mu$ 1AB-KD-hNIS) cells. (B) MDCK-hNIS,  $\mu$ 1A-KD-hNIS,  $\mu$ 1B-KD-hNIS, and  $\mu$ 1AB-KD-hNIS cells were plated on polycarbonate filters and analyzed for the polarized distribution of NIS. Representative confocal immunofluorescence orthogonal xz plane views stained for NIS (red) and the apical glycoprotein gp135 (green) are shown. Scale bars, 10  $\mu$ m. (C) Cells plated on polycarbonate filters were analyzed for the polarized distribution of NIS by biotinylation. Representative Western blots of NIS, TfR,  $\alpha$ -Na<sup>+</sup>/K<sup>+</sup>-ATPase, and gp135 proteins in basolateral (BL) and apical (Ap) domains are shown. The upper part shows the quantification of the NIS signal in each domain as the percentage of the total PM protein (Ap+BL). (D) Quantification of NIS localization IC vs. PM (BL+Ap). In (C, D) data represent the mean  $\pm$  SD for at least three experiments. Differences vs. control (MDCK-hNIS) were considered significant: \* $p$  < 0.05; \*\* $p$  < 0.01. IC, intracellular; RT-qPCR, quantitative reverse transcription polymerase chain reaction.

These results suggest that AP-1A does not participate in NIS sorting, with the caveat that the degree of  $\mu$ 1A silencing was modest. In addition, it is known that AP-1B can compensate for the loss of available AP-1A.<sup>31</sup>

*Knockdown of the  $\mu$ 1B subunit of AP-1B missorts NIS at the apical membrane of polarized MDCK cells*

We next examined the role of the epithelial-specific AP-1B variant, which interacts through its  $\mu$ 1B subunit with conventional tyrosine-based and unconventional signals localized on the cytoplasmic tail of cargo proteins.<sup>30,31,36</sup> Confocal microscopy revealed an apical redistribution of NIS in  $\mu$ 1B-knockdown MDCK-hNIS cells ( $\mu$ 1B-KD-hNIS) that contrasted dramatically with its exclusive basolateral localization in control MDCK-hNIS cells (Fig. 3B). Nevertheless, the morphology of tight junctions (ZO-1) and adherens junctions ( $\beta$ -catenin) and polarization were preserved (Sup-

plementary Fig. S1). Biotinylation analysis confirmed a decrease in the steady-state basolateral polarity of NIS in  $\mu$ 1B-KD-hNIS cells (61%  $\pm$  15%) and an increase in apical polarity (39%  $\pm$  15%), which was accompanied by a decrease in the basolateral distribution of TfR (Fig. 3C). Conversely,  $\alpha$ -Na<sup>+</sup>/K<sup>+</sup>-ATPase and gp135 displayed normal polarity, in agreement with previous observations.<sup>28</sup>

Overall, these results show that AP-1B is likely involved in NIS sorting to the basolateral membrane.

*Double knockdown of  $\mu$ 1A and  $\mu$ 1B provokes severe NIS missorting and demonstrates the involvement of AP-1A in basolateral NIS trafficking*

Our findings so far suggest that only AP-1B mediates NIS basolateral sorting. However, it is known that AP-1B can compensate for AP-1A function during basolateral sorting and membrane targeting of TfR and the low-density lipoprotein



(LDL)-receptor.<sup>31</sup> To clarify the role of AP-1A in NIS basolateral trafficking, we analyzed the polarized distribution of NIS in cells silenced for both  $\mu$ 1A and  $\mu$ 1B subunits ( $\mu$ 1AB-KD-hNIS) (Fig. 3). Confocal microscopy revealed strong apical NIS staining and colocalization with gp135 (Fig. 3B), and biotinylation assays demonstrated that 43%  $\pm$  5% of NIS was at the basolateral domain in  $\mu$ 1AB-KDhNIS cells, whereas 57%  $\pm$  5% was apically mistargeted (Fig. 3C). Conversely, TfR,  $\alpha$ -Na<sup>+</sup>/K<sup>+</sup>-ATPase, and gp135 localization was unimpaired. The more conspicuous NIS delocalization in  $\mu$ 1AB-KD cells compared with  $\mu$ 1B-KD cells indicates that the AP-1A complex also participates in NIS basolateral sorting and mediates correct NIS polarized PM distribution through its  $\mu$ 1 subunit.

When we quantified the intracellular versus PM (basolateral+apical) localization of NIS (Fig. 3D), we found a small but significant increase in intracellular NIS (86.4%  $\pm$  2.1% vs. 81.5%  $\pm$  1.4%) in  $\mu$ 1AB-KD-hNIS cells compared with MDCK-hNIS cells (Fig. 3D), and a decrease of NIS in the PM (13.6%  $\pm$  2.1% vs. 18.5%  $\pm$  1.4%). This was also observed by immunofluorescence microscopy (Supplementary Fig. S2).

These results demonstrate that both AP-1A and AP-1B mediate NIS basolateral sorting at the TGN and at REs, and both are involved in NIS trafficking. Moreover, the decrease/absence of their expression reduces the amount of NIS reaching the PM.

#### Mislocalized NIS at the apical membrane is functional

Given that NIS mislocalization has been associated with impaired function,<sup>34</sup> we next questioned whether the api-

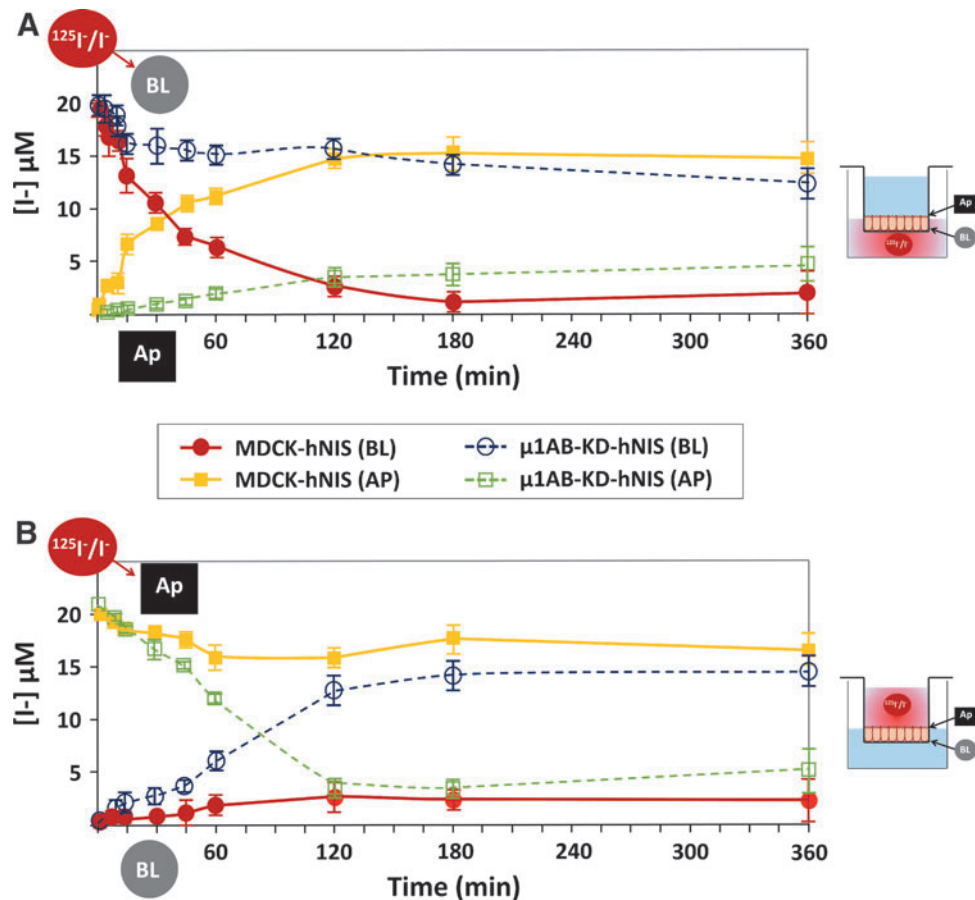
cally localized NIS remained functional and could transport iodide. We thus performed a timecourse iodide uptake assay in Transwell chambers using polarized MDCK-hNIS and  $\mu$ 1AB-KD-hNIS cells. Results showed that iodide added to the basolateral chamber was progressively transported to the apical chamber in MDCK-hNIS cells. By contrast, only a fraction of the iodide was transported from the basolateral to the apical chamber in  $\mu$ 1AB-KD-hNIS cells (Fig. 4A). We then evaluated the reverse reaction by adding iodide to the apical chamber.

Whereas little iodide was transported from the apical to the basolateral chamber in MDCK-hNIS cells, the bulk of iodide was transported from the apical to the basolateral chamber in  $\mu$ 1AB-KD-hNIS cells (Fig. 4B). The differences in the curve shape over time and in the amount of iodide transported by  $\mu$ 1AB-KD-hNIS (apical to basolateral) versus MDCK-hNIS (basolateral to apical) are presumably due to the occurrence of NIS on both sides of  $\mu$ 1AB-KD-hNIS cells. Overall, these results clearly demonstrate that the apically localized NIS is fully functional.

#### Analysis of NIS interactions with clathrin adaptor (AP-1A and AP-1B)

We next sought to determine the interaction between AP-1 subunits and NIS. We first performed *in silico* and manual searching for possible binding sites<sup>29,37</sup> using the proposed NIS topology (Fig. 5A, B).<sup>38–40</sup> We identified three sites within the intracellular loops and two sites at the C-terminus. Additionally, we inspected the functional involvement of the

**FIG. 4.** Apical-localized NIS is functional in  $\mu$ 1AB-KD-hNIS cells. Vectorial iodide transport in fully polarized MDCK-hNIS and  $\mu$ 1AB-KD-hNIS cells was measured in both chambers at the indicated time points. Iodide (20  $\mu$ M) supplemented with <sup>125</sup>I (100 mCi/mmol I) was added to the (A) basolateral (BL) or (B) apical (Ap) chamber, and 10  $\mu$ L of medium was collected from each chamber at the time points shown. Radioactivity was quantified and iodide concentration was determined. Two different experiments with replicates were performed. BL (red line, solid circles) and Ap (yellow line, solid squares) iodide concentration in MDCK-hNIS cells. BL (dotted blue line, empty circles) and Ap (dotted green line, empty squares) iodide concentration in  $\mu$ 1AB-KD-hNIS cells.



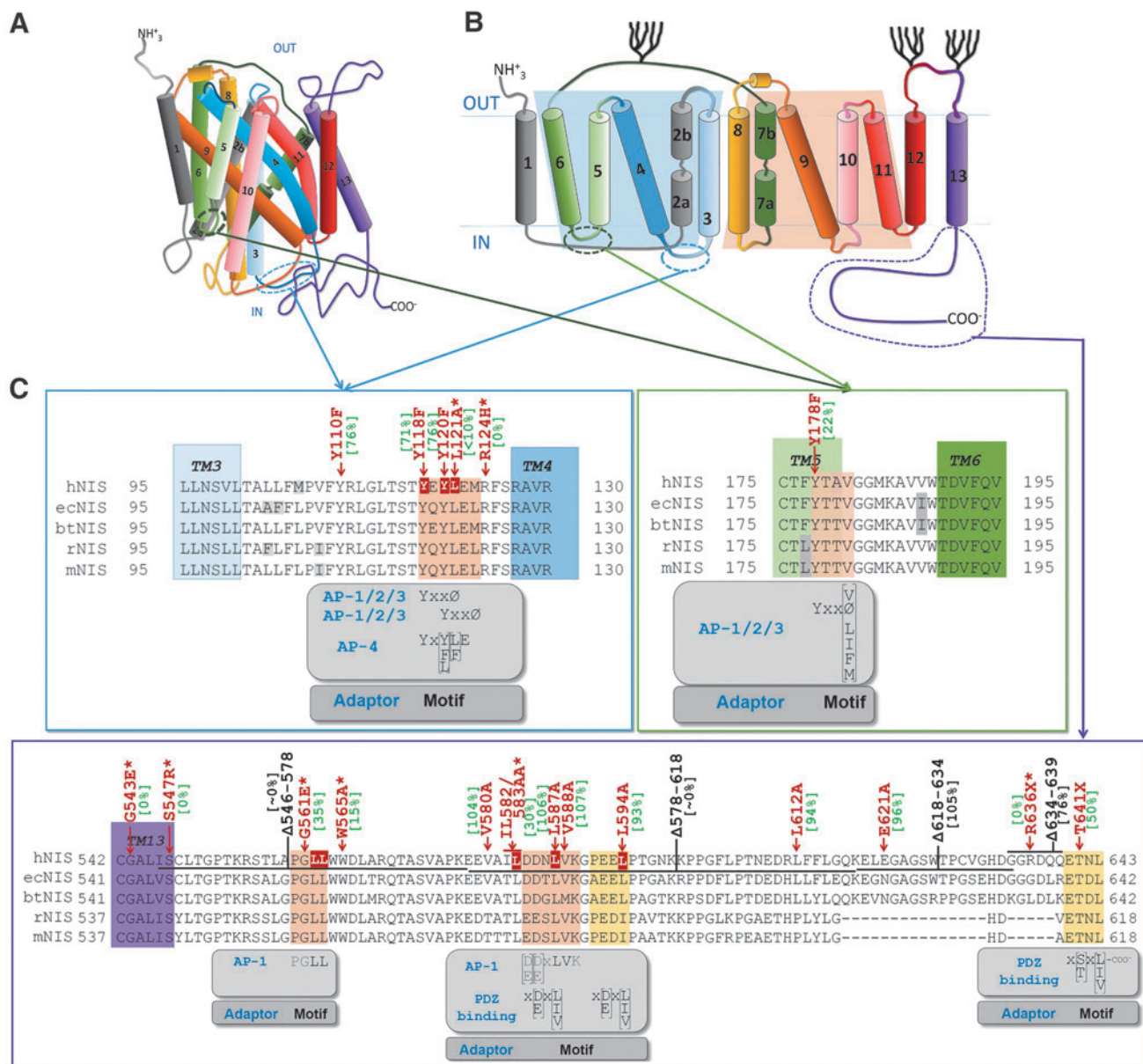


**FIG. 5.** *In silico* localization of the clathrin adaptor binding sites in the cytoplasmic region of NIS protein, and functional implications. (A) Proposed 3D topology of NIS based on the crystal structure of *Vibrio parahaemolyticus* sodium/galactose symporter crystal structure.<sup>40</sup> (B) NIS secondary structure model based on experimental findings.<sup>38,39</sup> (C) Putative binding sites localize to the intracellular region and within the intracellular C-terminal region. We detected three tyrosine-based putative motifs in the intracellular loops. Motifs fitted the minimal consensus for YxxØ signals (where Ø is a bulky hydrophobic residue and X any amino acid) that are known to bind to the  $\mu$ 1A/ $\mu$ 1B subunits of AP-1A and AP-1B complexes, respectively.<sup>30</sup> Two were localized in the intracellular region between the NIS TD 3 and 4: Y118[QE]YL121 and Y120LE[LM]123. The third was found at Y178T[AT]V181, between TD 5 and 6; however, these residues seem to be part of the TD6 helix according to the predicted model. Putative basolateral motifs that can be recognized by AP-1 were found in the C-terminal region: (i) a conserved dileucine motif PGLL (L562–L563), not previously reported<sup>25,32</sup>, and (ii) an LVK leucine-based motif preceded by a region of acidic residues, similar to the ALVVHP motif of syntaxin 4 that is responsible for its AP-1B-dependent basolateral localization.<sup>57</sup> The amino acid binding sites are indicated by an orange square in NIS. The corresponding motif and the possible adaptors are indicated below the sequence. Residues of NIS that have been mutated and functionally analyzed are indicated over the amino acid sequence (red), together with the percentage of activity (green square).<sup>3,25,32,34,41,54</sup> C-terminal deletions are also indicated (black). Additionally, an asterisk denotes that the indicated mutation has been determined to cause partial or total NIS mislocalization. AP-1, adaptor protein 1; TD, transmembrane domains.

surrounding region of those residues (Fig. 5C). Residues L121 and R124 in the loop between transmembrane domain 3 and 4 and C-terminal residues G561E, W565, and IL582/583AA disrupt NIS function,<sup>25,41</sup> making them good candidates for interaction. Indeed, a previous computational simulation analysis predicted an interaction between NIS residue L583 and AP-1B.<sup>32</sup>

We found an interaction between endogenous NIS and AP-1A/B subunits in PCC13 cells by co-immunoprecipitation (Fig. 6A). Importantly, clathrin was also part of this protein complex.

We cotransfected COS-7 cells with wild-type hNIS and with mutations at residues Y118A, Y120A, L121A, LL562/563AA, L583A, L587A and L594A, plus  $\mu$ 1A (AP1M1) or  $\mu$ 1B (AP1M2) cDNAs to determine the specific binding sites of this interaction. Immunoprecipitation analysis with antibodies to  $\mu$ 1A/B revealed the presence of hNIS in almost all cases; however, the amount of NIS observed in the immunoprecipitated complexes with the point mutations differed according to the mutant analyzed (Fig. 6B). Specifically, the presence of hNIS protein in the  $\mu$ 1A immunoprecipitate was less in the case of the L121A and L583A mutants, and almost undetectable in the LL562/563AA double mutant (Fig. 6C). In the  $\mu$ 1B immunoprecipitates, the interaction was weaker in the LL562/563AA double mutant and in the L583A mutant, although to a lesser extent (Fig. 6C). These findings indicate that the aforementioned mutations do not completely block the interaction between NIS and AP-1A/B subunits, suggesting that binding relies on more than one site.

Taken together, our results demonstrate that AP-1A/B interacts with NIS in both endogenous and exogenous systems, polarized or not, and highlight the likely importance of the hNIS residues L121, LL562/563, and L583 for this interaction.

## Discussion

NIS is essential in thyroid physiology and forms the basis of RAI therapy.<sup>3,4,42</sup> This therapy is, however, ineffective in some patients due to loss of NIS expression at both the level of mRNA<sup>43,44</sup> and protein, and to intracellular retention,<sup>7,10,45</sup> which may be caused by perturbations in NIS trafficking. When this occurs, patients are classified as RAI refractory. Nevertheless, given the success of RAI therapy in well-differentiated thyroid tumors, numerous targeted therapy strategies use NIS as a theragnostic tool.<sup>3,4,46,47</sup> While the biological function of NIS in thyroid and non-thyroid tissues is well characterized, the mechanisms controlling its sorting and subcellular distribution have not been sufficiently explored. Accordingly, a better understanding of these processes should facilitate improvements in RAI-based therapies.

Basolateral sorting of integral membrane proteins is directed primarily by signals located in the cytoplasmic domain of the sorted protein.<sup>22</sup> The heterotetrameric clathrin adaptor AP-1 has been implicated in basolateral sorting.<sup>48,49</sup> AP-1A/B can function either at the TGN or in REs depending on where they encounter their preferred cargo. Using confocal microscopy, we show that AP-1A/B demonstrates comparable localization with NIS in PCC13 cells. Indeed, they colocalize to similar extents with TGN/RE markers within the NIS trafficking route.

Loss of function, biotinylation, and confocal microscopy analysis reveal that AP-1A/B participate in NIS basolateral trafficking, although the role of AP-1A can be compensated by AP-1B. This phenomenon has been observed for basolateral sorting of the TfR and LDL receptors.<sup>31</sup> The absence of both AP-1A/B subunits led to mislocalized basolateral NIS in MDCK cells, with a dominant apical expression, and also to a decrease in total NIS localized to the PM.

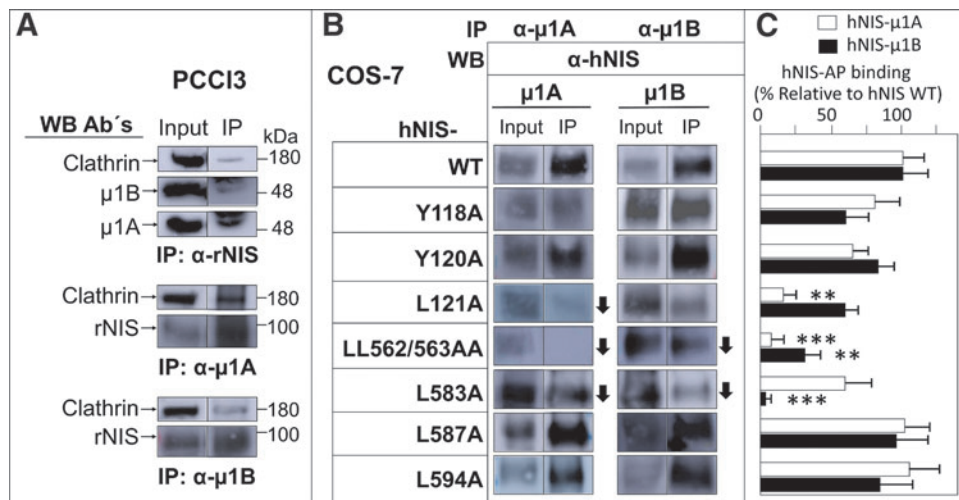


**FIG. 6.** Analysis of NIS interaction with clathrin-dependent  $\mu$ 1A and  $\mu$ 1B. (A) Western blotting using the indicated antibodies (left) against PCC13 input or IP complexes with rNIS (top),  $\mu$ 1A (middle), or  $\mu$ 1B (bottom) antibodies. (B) Western blotting of COS-7 cells cotransfected with WT hNIS or the indicated mutants (left) and with  $\mu$ 1A or  $\mu$ 1B, as indicated. Following IP with  $\mu$ 1A or  $\mu$ 1B, extracts were immunoblotted with a rabbit polyclonal anti-hNIS antibody. Input or IP fractions are indicated. The arrows highlight a decrease in the signal when compared with WT hNIS. The bands shown for each IP and Western blot are from the same membrane but were separated in the original Western blot. Western blots are representative of at least two experiments. (C) Estimation of the interaction of  $\mu$ 1A or  $\mu$ 1B with hNIS. The NIS signal obtained in the IP fraction was standardized to the input and then normalized to the interaction observed in the hNIS WT protein. Data represent the mean  $\pm$  SD of at least three experiments. Differences vs. control (MDCK-hNIS WT) were considered significant: \*\* $p < 0.01$ ; \*\*\* $p < 0.001$ . IP, immunoprecipitated; WT, wild type.



Using bioinformatics and manual searching, we found five putative binding sites for clathrin adaptor proteins (Fig. 5). Importantly, mutations in residues in the loop between transmembrane domains 3–4 have been previously implicated in NIS function and localization.<sup>41</sup>

The finding that NIS trafficking is clathrin-mediated might explain its different tissue-related location. The  $\mu$ 1A subunit is expressed in all cells,<sup>50–52</sup> whereas the  $\mu$ 1B isoform is expressed differentially in some mammalian epithelial cells (e.g., distal kidney) where NIS localizes basolaterally,<sup>4,7</sup> but not in other epithelial cells (e.g., kidney proximal cells) where NIS localizes apically.<sup>4,6</sup>

We also show that apically expressed NIS is functional following the elimination of the  $\mu$ 1AB isoform and can participate in iodide uptake from the apical space. Accordingly, NIS located apically in the proximal tube could participate in iodide reabsorption, as has been predicted.<sup>4</sup>

Site-directed mutagenesis and co-immunoprecipitation allowed us to identify the specific NIS residues that interact with  $\mu$ 1A (L121 and LL562/563) and  $\mu$ 1B (L583 and LL562/563). In most cases, the amino acid substitution did not completely abolish the interaction between NIS and AP-1. This is common to this type of approach<sup>53</sup> and can be explained by the fact that the mutation only partially reduces binding affinity, or it might suggest the presence of multiple interaction sites. A previous study described that the C-terminus of NIS is involved in its trafficking (Fig. 5). A tryptophan acidic motif around W565 was suggested to interact with kinesin-1 light chain-2,<sup>54</sup> in a region close to LL562/563, which are critical residues for  $\mu$ 1A binding as shown here. Also, by a modeling approach, they tentatively identified an interaction between  $\mu$ 1B and the L583 residue.<sup>32</sup> Here, we confirm this interaction experimentally and provide a detailed map of the NIS residues involved in clathrin adaptor binding.

Our characterization of NIS sorting and trafficking allows us to propose the following mechanism. After NIS synthesis in REs and total glycosylation in the Golgi apparatus, in polarized cells AP-1 adaptors bind NIS in the TGN, where AP-1A-enriched vesicles sort NIS directly to the PM. In addition, AP-1B-enriched vesicles translocate to REs and sort NIS to the PM in a clathrin-dependent mechanism (Fig. 7). In non-polarized cells, AP-1A/B contributes to NIS PM sorting.

These findings advance our understanding of NIS trafficking not only in epithelial cells in physiological conditions but also in non-polarized cells of refractory thyroid carcinomas where NIS fails to reach the PM and, hence, loses the ability to concentrate RAI. It will be important to analyze whether AP-1A/B proteins are altered in thyroid cancer. As a prelude to this analysis, we used the GEPIA webserver<sup>55</sup> to perform a differential gene analysis of NIS (*SLC5A5*),  $\mu$ 1A (*AP1M1*), and  $\mu$ 1B (*AP1M2*) in samples of the Thyroid Cancer Genome Atlas.<sup>56</sup> We found that *SLC5A5* and *AP1M1* are downregulated in tumor samples, and *AP1M2* is upregulated with respect to control tissue (Supplementary Fig. S3). Additionally, we found a positive correlation between *SLC5A5* and both *AP1M1* and *ARF4*, another clathrin-dependent factor involved in NIS trafficking.<sup>23</sup> Therefore, AP-1A/B might be a new target to increase NIS trafficking to the PM and improve RAI therapy in patients with refractory thyroid cancer.

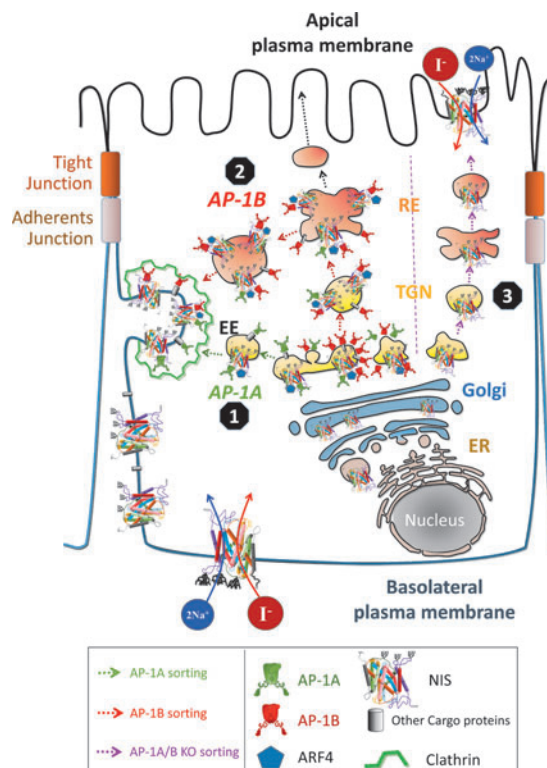


**FIG. 7.** Model of NIS trafficking in epithelial cells. The AP complexes are widely distributed throughout the post-Golgi network. ① Ubiquitously expressed AP-1A is localized at the TGN and endosomes and regulates TGN-endosomal sorting and may directly regulate NIS TGN-basolateral PM sorting (AP-1A sorting, indicated in green lines). ② Epithelium-specific AP-1B is localized at the TGN and/or at the recycling endosomes and is crucial for the control of polarized NIS sorting to the basolateral PM (AP-1B sorting, indicated in red lines). ARF4 may be part of the clathrin-coated vesicles. ③ Accordingly, the cargo (NIS) can be sorted to the lysosomal compartment or recycling. In the absence of AP-1A/B, NIS is delivered to the apical membrane (AP-1A/B KO sorting, indicated in purple lines). ARF4, ADP ribosylation factor 4; EE, early endosome; ER, endoplasmic reticulum; RE, recycling endosome.

#### Authors' Contributions

P.K., C.F.-M., A.D.I.V., D.F.-D., and L.M.M. conducted the experiments. P.K. and A.D.I.V. analyzed the data and conducted bioinformatic analysis. P.K., C.F.-M., A.D.I.V., and P.S. designed the research and wrote the article.

#### Acknowledgments

We are grateful to Dr. Enrique Rodriguez-Boulan (Department of Cell and Developmental Biology, Weill Cornell Medical College, New York) for providing the MDCK cells with stable knockdown (KD) of the  $\mu$  subunit of AP-1B; to Dr. Heike Folsch (Department of Biochemistry, Molecular Biology, and Cell Biology, Northwestern University, Evanston) for the pBC6-mouse  $\mu$ 1A-HA and pBC6-human  $\mu$ 1B-HA expression vectors, and to Dr. Nancy Carrasco (Vanderbilt University, Nashville) for providing MDCK-hNIS cells, the pcDNA3.1(-)-hNIS expression vector, and NIS antibodies. We thank to Dr. Daniela Corda

(Institute of Protein Biochemistry-IPF, CNR, Naples) for supporting P.K. in her predoctoral training and Dr. Kenneth McCreath for helpful comments on the article. Some of the results included in this study were reported in the PhD thesis of P.K.

#### Author Disclosure Statement

No competing financial interests exist.

#### Funding Information

This work was supported by grants PID2019-105303RB I00/AEI/10.13039/501100011033 from Ministerio de Ciencia e Innovación (MICIN) and B2017/BMD-3724, Tironet2-CM from Comunidad de Madrid (Spain) to P.S.; and SAF2015-69964-R, RTI2018-099343-B-100 from the MICIN, Spain, and Fondo Europeo de Desarrollo Regional to A.D.I.V. P.S. and A.D.I.V. laboratories are supported jointly by CIBERONC CB16/12/00326 from the Instituto de Salud Carlos III (ISCIII). P.K., C.F.-M., and L.M.M. held predoctoral fellowship from Ministerio de Economía y Competitividad, Universidad Autónoma de Madrid (Spain) and CIBERONC, respectively. D.F.-D. holds a contract associated with Grant SAF2015-69964-R.

#### Supplementary Material

Supplementary Data

#### References

- De La Vieja A, Dohan O, Levy O, et al. Molecular analysis of the sodium/iodide symporter: Impact on thyroid and extrathyroid pathophysiology. *Physiol Rev* 2000;80(3):1083–1105; doi: 10.1152/physrev.2000.80.3.1083.
- Riesco-Eizaguirre G, Leoni SG, Mendiola M, et al. NIS mediates iodide uptake in the female reproductive tract and is a poor prognostic factor in ovarian cancer. *J Clin Endocrinol Metab* 2014;99(7):E1199–E1208; doi: 10.1210/jc.2013-4249.
- Ravera S, Reyna-Neyra A, Ferrandino G, et al. The sodium/iodide symporter (NIS): Molecular physiology and pre-clinical and clinical applications. *Annu Rev Physiol* 2017;79:261–289; doi: 10.1146/annurev-physiol-022516-034125.
- De la Vieja A, Santisteban P. Role of iodide metabolism in physiology and cancer. *Endocr Relat Cancer* 2018;25(4):R225–R245; doi: 10.1530/ERC-17-0515.
- Mitsuma T, Rhue N, Hirooka Y, et al. Organ distribution of iodide transporter (symporter) in the rat: Immunohistochemical study. *Endocr Regul* 1997;31(1):15–18.
- Spitzweg C, Dutton CM, Castro MR, et al. Expression of the sodium iodide symporter in human kidney. *Kidney Int* 2001;59(3):1013–1023; doi: 10.1046/j.1523-1755.2001.0590031013.x.
- Wapnir IL, van de Rijn M, Nowels K, et al. Immunohistochemical profile of the sodium/iodide symporter in thyroid, breast, and other carcinomas using high density tissue microarrays and conventional sections. *J Clin Endocrinol Metab* 2003;88(4):1880–1888; doi: 10.1210/jc.2002-021544.
- Nicola JP, Basquin C, Portulano C, et al. The Na<sup>+</sup>/I<sup>-</sup> symporter mediates active iodide uptake in the intestine. *Am J Physiol Cell Physiol* 2009;296(4):C654–C662; doi: 10.1152/ajpcell.00509.2008.
- Riesco-Eizaguirre G, Santisteban P, De la Vieja A. The complex regulation of NIS expression and activity in thyroid and extrathyroidal tissues. *Endocr Relat Cancer* 2021;28(10):T141–T165; doi: 10.1530/ERC-21-0217.
- Tavares C, Coelho MJ, Eloy C, et al. NIS expression in thyroid tumors, relation with prognosis clinicopathological and molecular features. *Endocr Connect* 2018;7(1):78–90; doi: 10.1530/EC-17-0302.
- Riedel C, Levy O, Carrasco N. Post-transcriptional regulation of the sodium/iodide symporter by thyrotropin. *J Biol Chem* 2001;276(24):21458–21463; doi: 10.1074/jbc.M100561200.
- Kogai T, Endo T, Saito T, et al. Regulation by thyroid-stimulating hormone of sodium/iodide symporter gene expression and protein levels in FRTL-5 cells. *Endocrinology* 1997;138(6):2227–2232; doi: 10.1210/endo.138.6.5189.
- Leoni SG, Kimura ET, Santisteban P, et al. Regulation of thyroid oxidative state by thioredoxin reductase has a crucial role in thyroid responses to iodide excess. *Mol Endocrinol* 2011;25(11):1924–1935; doi: 10.1210/me.2011-0038.
- Leoni SG, Sastre-Perona A, De la Vieja A, et al. Selenium increases thyroid-stimulating hormone-induced sodium/iodide symporter expression through thioredoxin/apurinic/aprimidinic endonuclease 1-dependent regulation of paired box 8 binding activity. *Antioxid Redox Signal* 2016;24(15):855–866; doi: 10.1089/ars.2014.6228.
- Eng PH, Cardona GR, Previti MC, et al. Regulation of the sodium iodide symporter by iodide in FRTL-5 cells. *Eur J Endocrinol* 2001;144(2):139–144; doi: 10.1530/eje.0.1440139.
- Riesco-Eizaguirre G, Rodriguez I, De la Vieja A, et al. The BRAFV600E oncogene induces transforming growth factor beta secretion leading to sodium iodide symporter repression and increased malignancy in thyroid cancer. *Cancer Res* 2009;69(21):8317–8325; doi: 10.1158/0008-5472.CAN-09-1248.
- Knauf JA, Fagin JA. Role of MAPK pathway oncoproteins in thyroid cancer pathogenesis and as drug targets. *Curr Opin Cell Biol* 2009;21(2):296–303; doi: 10.1016/j.ceb.2009.01.013.
- Hou P, Bojdani E, Xing M. Induction of thyroid gene expression and radioiodine uptake in thyroid cancer cells by targeting major signaling pathways. *J Clin Endocrinol Metab* 2010;95(2):820–828; doi: 10.1210/jc.2009-1888.
- Lacoste C, Herve J, Bou Nader M, et al. Iodide transporter NIS regulates cancer cell motility and invasiveness by interacting with the Rho guanine nucleotide exchange factor LARG. *Cancer Res* 2012;72(21):5505–5515; doi: 10.1158/0008-5472.CAN-12-0516.
- Stratford AL, Boelaert K, Tannahill LA, et al. Pituitary tumor transforming gene binding factor: A novel transforming gene in thyroid tumorigenesis. *J Clin Endocrinol Metab* 2005;90(7):4341–4349; doi: 10.1210/jc.2005-0523.
- Smith VE, Read ML, Turnell AS, et al. A novel mechanism of sodium iodide symporter repression in differentiated thyroid cancer. *J Cell Sci* 2009;122(Pt 18):3393–3402; doi: 10.1242/jcs.045427.
- Fletcher A, Read ML, Thornton CEM, et al. Targeting novel sodium iodide symporter interactors ADP-ribosylation factor 4 and valosin-containing protein enhances radio-

- iodine uptake. *Cancer Res* 2020;80(1):102–115; doi: 10.1158/0008-5472.CAN-19-1957.
23. Kim SK. Polarized signaling: Basolateral receptor localization in epithelial cells by PDZ-containing proteins. *Curr Opin Cell Biol* 1997;9(6):853–859; doi: 10.1016/s0955-0674(97)80088-9.
  24. Darrouzet E, Graslin F, Marcellin D, et al. A systematic evaluation of sorting motifs in the sodium-iodide symporter (NIS). *Biochem J* 2016;473(7):919–928; doi: 10.1042/BJ20151086.
  25. Dohan O, De la Vieja A, Paroder V, et al. The sodium/iodide Symporter (NIS): Characterization, regulation, and medical significance. *Endocr Rev* 2003;24(1):48–77; doi: 10.1210/er.2001-0029.
  26. Bonifacino JS. Adaptor proteins involved in polarized sorting. *J Cell Biol* 2014;204(1):7–17; doi: 10.1083/jcb.201310021.
  27. Folsch H, Pypaert M, Schu P, et al. Distribution and function of AP-1 clathrin adaptor complexes in polarized epithelial cells. *J Cell Biol* 2001;152(3):595–606; doi: 10.1083/jcb.152.3.595.
  28. Gravotta D, Deora A, Perret E, et al. AP1B sorts basolateral proteins in recycling and biosynthetic routes of MDCK cells. *Proc Natl Acad Sci U S A* 2007;104(5):1564–1569; doi: 10.1073/pnas.0610700104.
  29. Gonzalez A, Rodriguez-Boulan E. Clathrin and AP1B: Key roles in basolateral trafficking through trans-endosomal routes. *FEBS Lett* 2009;583(23):3784–3795; doi: 10.1016/j.febslet.2009.10.050.
  30. Carvajal-Gonzalez JM, Gravotta D, Mattera R, et al. Basolateral sorting of the coxsackie and adenovirus receptor through interaction of a canonical YXXPhi motif with the clathrin adaptors AP-1A and AP-1B. *Proc Natl Acad Sci U S A* 2012;109(10):3820–3825; doi: 10.1073/pnas.1117949109.
  31. Gravotta D, Carvajal-Gonzalez JM, Mattera R, et al. The clathrin adaptor AP-1A mediates basolateral polarity. *Dev Cell* 2012;22(4):811–823; doi: 10.1016/j.devcel.2012.02.004.
  32. Martin M, Modenutti CP, Peyret V, et al. A carboxy-terminal monoleucine-based motif participates in the basolateral targeting of the Na<sup>+</sup>/I<sup>-</sup> symporter. *Endocrinology* 2019;160(1):156–168; doi: 10.1210/en.2018-00603.
  33. Riesco-Eizaguirre G, De la Vieja A, Rodriguez I, et al. Telomerase-driven expression of the sodium iodide symporter (NIS) for in vivo radioiodide treatment of cancer: A new broad-spectrum NIS-mediated antitumor approach. *J Clin Endocrinol Metab* 2011;96(9):E1435–E1443; doi: 10.1210/jc.2010-2373.
  34. De la Vieja A, Ginter CS, Carrasco N. Molecular analysis of a congenital iodide transport defect: G543E impairs maturation and trafficking of the Na<sup>+</sup>/I<sup>-</sup> symporter. *Mol Endocrinol* 2005;19(11):2847–2858; doi: 10.1210/me.2005-0162.
  35. Ang AL, Taguchi T, Francis S, et al. Recycling endosomes can serve as intermediates during transport from the Golgi to the plasma membrane of MDCK cells. *J Cell Biol* 2004;167(3):531–543; doi: 10.1083/jcb.200408165.
  36. Guo X, Mattera R, Ren X, et al. The adaptor protein-1 mu1B subunit expands the repertoire of basolateral sorting signal recognition in epithelial cells. *Dev Cell* 2013;27(3):353–366; doi: 10.1016/j.devcel.2013.10.006.
  37. Janvier K, Kato Y, Boehm M, et al. Recognition of dileucine-based sorting signals from HIV-1 Nef and LIMP-II by the AP-1 gamma-sigma1 and AP-3 delta-sigma3 hemi-complexes. *J Cell Biol* 2003;163(6):1281–1290; doi: 10.1083/jcb.200307157.
  38. Levy O, De la Vieja A, Ginter CS, et al. N-linked glycosylation of the thyroid Na<sup>+</sup>/I<sup>-</sup> symporter (NIS). Implications for its secondary structure model. *J Biol Chem* 1998;273(35):22657–22663; doi: 10.1074/jbc.273.35.22657.
  39. De la Vieja A, Reed MD, Ginter CS, et al. Amino acid residues in transmembrane segment IX of the Na<sup>+</sup>/I<sup>-</sup> symporter play a role in its Na<sup>+</sup> dependence and are critical for transport activity. *J Biol Chem* 2007;282(35):25290–25298; doi: 10.1074/jbc.M700147200.
  40. Faham S, Watanabe A, Besserer GM, et al. The crystal structure of a sodium galactose transporter reveals mechanistic insights into Na<sup>+</sup>/sugar symport. *Science* 2008;321(5890):810–814; doi: 10.1126/science.1160406.
  41. Paroder V, Nicola JP, Ginter CS, et al. The iodide-transport-defect-causing mutation R124H: A delta-amino group at position 124 is critical for maturation and trafficking of the Na<sup>+</sup>/I<sup>-</sup> symporter. *J Cell Sci* 2013;126(Pt 15):3305–3313; doi: 10.1242/jcs.120246.
  42. Riesco-Eizaguirre G, Santisteban P. New insights in thyroid follicular cell biology and its impact in thyroid cancer therapy. *Endocr Relat Cancer* 2007;14(4):957–977; doi: 10.1677/ERC-07-0085.
  43. Bastos AU, Oler G, Nozima BH, et al. BRAF V600E and decreased NIS and TPO expression are associated with aggressiveness of a subgroup of papillary thyroid microcarcinoma. *Eur J Endocrinol* 2015;173(4):525–540; doi: 10.1530/EJE-15-0254.
  44. Lazar V, Bidart JM, Caillou B, et al. Expression of the Na<sup>+</sup>/I<sup>-</sup> symporter gene in human thyroid tumors: A comparison study with other thyroid-specific genes. *J Clin Endocrinol Metab* 1999;84(9):3228–3234; doi: 10.1210/jcem.84.9.5996.
  45. Sodre AK, Rubio IG, Galrao AL, et al. Association of low sodium-iodide symporter messenger ribonucleic acid expression in malignant thyroid nodules with increased intracellular protein staining. *J Clin Endocrinol Metab* 2008;93(10):4141–4145; doi: 10.1210/jc.2007-0353.
  46. Miller A, Russell SJ. The use of the NIS reporter gene for optimizing oncolytic virotherapy. *Expert Opin Biol Ther* 2016;16(1):15–32; doi: 10.1517/14712598.2016.1100162.
  47. Spitzweg C, Harrington KJ, Pinke LA, et al. Clinical review 132: The sodium iodide symporter and its potential role in cancer therapy. *J Clin Endocrinol Metab* 2001;86(7):3327–3335; doi: 10.1210/jcem.86.7.7641.
  48. Nakatsu F, Ohno H. Adaptor protein complexes as the key regulators of protein sorting in the post-Golgi network. *Cell Struct Funct* 2003;28(5):419–429; doi: 10.1247/csf.28.419.
  49. Robinson MS. Forty years of clathrin-coated vesicles. *Traffic* 2015;16(12):1210–1238; doi: 10.1111/tra.12335.
  50. Diaz F, Gravotta D, Deora A, et al. Clathrin adaptor AP1B controls adenovirus infectivity of epithelial cells. *Proc Natl Acad Sci U S A* 2009;106(27):11143–11148; doi: 10.1073/pnas.0811227106.
  51. Ohno H, Tomemori T, Nakatsu F, et al. Mu1B, a novel adaptor medium chain expressed in polarized epithelial cells. *FEBS Lett* 1999;449(2–3):215–220; doi: 10.1016/s0014-5793(99)00432-9.
  52. Schreiner R, Frindt G, Diaz F, et al. The absence of a clathrin adapter confers unique polarity essential to proximal tubule function. *Kidney Int* 2010;78(4):382–388; doi: 10.1038/ki.2010.166.



53. Xiao F, Wang S, Barouch-Bentov R, et al. Interactions between the hepatitis C virus nonstructural 2 protein and host adaptor proteins 1 and 4 orchestrate virus release. *mBio* 2018;9(2):e02233-17; doi: 10.1128/mBio.02233-17.
54. Martin M, Modenutti CP, Gil Rosas ML, et al. A novel SLC5A5 variant reveals the crucial role of kinesin light chain 2 in thyroid hormonogenesis. *J Clin Endocrinol Metab* 2021;106(7):1867–1881; doi: 10.1210/clinem/dgab283.
55. Tang Z, Li C, Kang B, et al. GEPIA: A web server for cancer and normal gene expression profiling and interactive analyses. *Nucleic Acids Res* 2017;45(W1):W98–W102; doi: 10.1093/nar/gkx247.
56. Cancer Genome Atlas Research Network. Integrated genomic characterization of papillary thyroid carcinoma. *Cell* 2014;159(3):676–690; doi: 10.1016/j.cell.2014.09.050.
57. Reales E, Sharma N, Low SH, et al. Basolateral sorting of syntaxin 4 is dependent on its N-terminal domain and the AP1B clathrin adaptor, and required for the epithelial cell polarity. *PLoS One* 2011;6(6):e21181; doi: 10.1371/journal.pone.0021181.

Address correspondence to:

*Pilar Santisteban, PhD*  
*Instituto de Investigaciones Biomédicas “Alberto Sols”*  
*Consejo Superior de Investigaciones Científicas*  
*Universidad Autónoma de Madrid*  
*C/Arturo Duperier 4*  
*Madrid 28029*  
*Spain*

*E-mail: psantisteban@iib.uam.es*

*Antonio De la Vieja, PhD*  
*Unidad de Tumores Endocrinos (UFIEC)*  
*Instituto de Salud Carlos III (ISCIII)*  
*Ctra. Majadahonda-Pozuelo km 2,2.*  
*Majadahonda (Madrid) 28220*  
*Spain*

*E-mail: adelavieja@isciii.es*